

3. DEPOSITIONAL ENVIRONMENT AND PETROGRAPHY OF PREGLACIAL CONTINENTAL SEDIMENTS FROM HOLE 740A, PRYDZ BAY, EAST ANTARCTICA¹

Brian R. Turner²

ABSTRACT

ODP Hole 740A is located on the inner part of the East Antarctic continental shelf in Prydz Bay, at the seaward end of a major onshore rift structure known as the Lambert Graben. Drilling at this site led to the recovery of some 65 m of continental sediments (Prydz Bay red beds) that form part of a much thicker (2–3 km) pre-continental breakup sequence, the development of which may be related to the initiation and rifting of the Lambert Graben. Palynological and paleomagnetic studies have not been able to determine the age of the sediments; they may be equivalent to the onshore late Permian Amery Group or younger. The succession consists predominantly of sandstone, siltstone, and claystone arranged in erosively based, pedogenically influenced fining-upward sequences up to 5 m thick. These were deposited by shallow, braided streams draining an extensively vegetated alluvial plain, with sufficient topographic relief to trap fine-grained sediment and inhibit rapid channel shifting. Pedogenic processes were initiated on the alluvial plain, but climatic conditions were generally unsuitable for extensive pedogenic carbonate formation and the development of mature soil profiles. The sediments were probably derived from a rapidly uplifted fault block terrain composed of upper Proterozoic and Archaean gneisses lying to the southeast of the depositional site. Uplift may have taken place along the tectonically active seaward extension of the eastern faulted margin of the Lambert Graben, which passes immediately southeast of Hole 740A. Differences in mineralogical composition between the Amery Group and the Prydz Bay red beds probably reflect differences in rock composition in the source area. The age of the Prydz Bay red beds has still to be resolved.

INTRODUCTION

Ocean Drilling Program (ODP) Leg 119 drilled five sites on the East Antarctic continental shelf in Prydz Bay, which lies at the seaward end of a major onshore rift structure known as the Lambert Graben (Fig. 1) (Stagg, 1985; Barron, Larsen, et al., 1989). Encountered in the innermost Hole 740A was a thin cover of glacial and glaciomarine sediments (~56 m) underlain by some 169 m of continental red beds, of which 65 m was recovered. The red beds lie some 300 m above the basement and when traced seaward they can be seen to form part of a 2–3-km-thick subhorizontal sequence of continental and possibly shallow-water marine sediments containing a major seismically defined unconformity that may separate prebreakup and post-breakup sediments. They represent part of the prebreakup sequence beneath the unconformity, the development of which was probably related to the initiation and rifting of the Lambert Graben, prior to the Indo-Antarctic breakup in the early Neocomian (Stagg, 1985). The red beds at this hole represent the first record of prebreakup sequence sediments known from primary (core) data.

SEDIMENTARY SUCCESSION

Description

The sediments at Hole 740A consist of sandstone interbedded with siltstone and claystone. The ratio of sandstone to siltstone and claystone decreases markedly toward the top of the succession, from 2/1 in the lower part to 1/1.6 in the upper part (Fig. 2). Internally the succession is characterized by fining-up-

ward and subordinate coarsening-upward sequences up to 5 m thick. However, because of poor core recovery at this site, relatively few sequences are complete. Individual fining-upward sequences are erosively based and composed of sandstone sharply overlain by siltstone and claystone (Fig. 3). The erosion surface at the base of the sequence appears to be generally of low relief and locally overlain by a thin, matrix-supported conglomerate containing angular to subangular, elongate claystone and siltstone intraclasts up to 3.5 cm long and rounded to subrounded pebbles and granules of quartz, quartzite, gneiss, and granite, together with quartzo-feldspathic and rare basic metamorphic clasts (Barron, Larsen, et al., 1989, p. 354, fig. 8). The more elongate clasts show imbrication. One erosion surface cuts diagonally across the core at an angle of about 30° and is overlain by claystone intraclasts, including one very large clast up to 10 cm long (Fig. 4). The smaller, more elongate clasts have their long axes aligned parallel to the scour surface. Most of the externally derived clasts are concentrated in the lower part of the succession, thereby emphasizing the overall fining-upward trend (Fig. 2). This is further emphasized by the individual fining-upward sequences in the succession, which are mostly sandstone dominated in the lower part and siltstone and claystone dominated in the upper part.

The sandstones are red to greenish gray and medium to coarse grained, and they attain a maximum thickness of about 3 m. They show a distinct fining-upward trend, with the coarsest parts of the sandstone predominantly green or greenish gray (Fig. 2) owing to the abundance of chlorite and lack of oxidized iron. Both the greenish gray reduced sandstones and the red oxidized sandstones contain locally developed zones of contrasting color and redox potential. Some of the reduced zones in the red oxidized sandstones concentrate around dark, organic-rich cores such as rootlets. Small angular to subrounded pebbles and granules of quartz, quartzite, and feldspar are scattered throughout the sandstone or less commonly concentrated into discrete layers and stringers. Some of the more elongate pebbles and granules show a distinct horizontal fabric. Grains of pyrite are par-

¹ Barron, J., Larsen, B., et al., 1991. *Proc. ODP, Sci. Results*, 119: College Station, TX (Ocean Drilling Program).

² Department of Geology, The University, Newcastle Upon Tyne, NE1 7RU, U.K. (Present address: University of Durham, Department of Geological Sciences, Science Laboratories, South Road, Durham, DH1 3LE, U.K.).

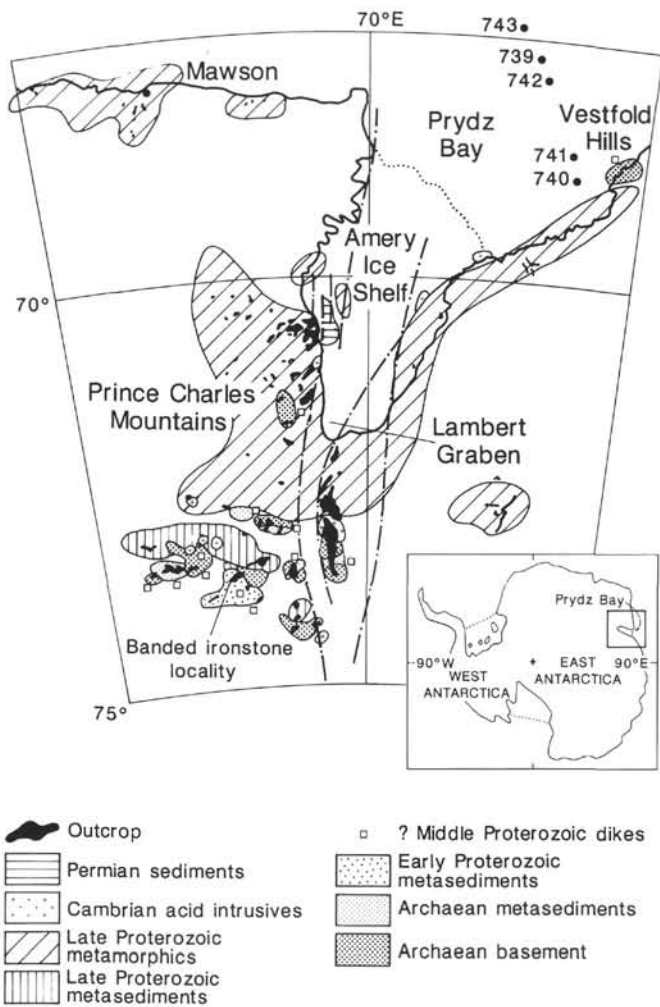


Figure 1. Generalized geologic map of the Prydz Bay area showing the location of the Lambert Graben and drill sites on the East Antarctic continental shelf.

ticularly common in the reduced greenish gray sandstones. Internal scouring of the sandstones is present in some parts of the core, but is not common.

The sandstones are simple, single-story sand bodies (Pettijohn et al., 1987). They may be massive or more commonly cross-bedded with minor ripple cross-lamination and horizontal lamination. The cross-bedding consists mainly of vertically stacked planar sets (Fig. 3); a single occurrence of trough cross-bedding is confined to a 0.50-m-thick sand body near the top of the succession (Fig. 3). The troughs are arranged in cosets, in which the individual sets are consistently about 4 cm thick (Barron, Larsen, et al., 1989, p. 355, fig. 10). Within the core, individual planar sets have straight upper and lower bounding surfaces typical of tabular cross-strata, although the lateral extent of these bounding surfaces is uncertain. Some of the sets show an upward decrease in set thickness from a maximum of about 1 to 0.05 m, concomitant with a similar decrease in grain size. The foreset laminae are texturally graded from coarse to fine and attain a maximum thickness of about 6 cm. Small pebbles and granules of quartz tend to concentrate along the base of the foresets. The foresets are typically straight and parallel to one another (Barron, Larsen, et al., 1989, p. 355, fig. 9) and inclined at angles of up to 25° to the lower planar bounding sur-

face, although most have lower foreset dip angles (<14°). Angular contact with this bounding surface is sharp and nonerosive with no evidence from the core of tangentially based foresets. In some sand bodies individual foreset laminae can be distinguished by their striped red and green appearance. The coarser laminae are typically green and greenish gray, whereas the finer laminae are more clay rich and red or pinkish gray in color.

Small-scale ripple cross-lamination, with amplitudes of form sets up to 1.5 cm and wavelengths up to 6 cm, is locally developed between cross-bedded units and in the finer grained upper parts of major sand bodies. In one example, cross-lamination dips in the opposite direction to that of the planar cross-beds above and below. A few ripples show clay-draped ripple profiles. These are located between a large-scale cross-bedded set and small-scale cosets where there is a sudden decrease in grain size (Fig. 2). Rare sigmoidal foreset laminae up to 0.7 cm thick and dipping at about 20° occur in Section 119-740A-26R-2, 56–60 cm. Most of the wavy lamination and horizontal lamination occur in the lower part of the more massive sandstones, which are locally mottled in shades of brown and yellowish brown. Spacing between individual laminae is on a millimeter to centimeter scale. In some parts of the core they can be differentiated on the basis of alternating red and green and light and dark red-colored laminae. In addition to the color-differentiated laminae, diagenetic red and green color banding is locally developed, in which the contrasting bands are sharply differentiated and range from 1.4 mm to 4 cm in thickness. Internally the red bands show a striking variation in color; some have a darker, fine red rim at the top, whilst others have more pale interiors. The texture between different color bands is the same throughout, in contrast to the sedimentary lamination. Mottled zones are less common than in the siltstone and claystone higher in the sequence.

The siltstone and claystone are predominantly red or reddish brown in color with numerous greenish gray reduction spots and lenses, some of which show dark organic-rich nuclei preserved in the center (Barron, Larsen, et al., 1989, p. 356, fig. 11). The claystone, which is subordinate to siltstone in most sequences, has a variable silt content. However, claystone coloration bears no significant relationship to stratification type or silt content. Both the siltstone and claystone contain coarser, more pale, diffuse sandy layers on a millimeter- to centimeter-thick scale and numerous claystone and siltstone intraclasts, locally concentrated into conglomerate lenses. Most intraclasts are small and less than 1.5 cm long. The largest intraclast recorded is a yellowish brown, striped siltstone up to 4.3 cm long. Internally, the siltstone and claystone show slickenside surfaces, some of which are coated with a thin claystone skin. Fining-upward sequences up to 25 cm thick occur within the siltstone and claystone. They consist of two main types: (1) fine sandstone and siltstone (sporadically rippled), passing up into claystone, and (2) erosively based intraformational conglomerate with a sandy matrix, passing up into finely laminated and locally rippled siltstone and claystone (Fig. 5). Small granules and large grains of subangular to subrounded quartz and feldspar up to 3 mm in length are sporadically distributed throughout the siltstone and claystone, which may also contain pyrite. This is particularly common in the siltstones, where the pyrite may be surrounded by a dark rim of organic-rich material. The siltstone and claystone are mainly structureless, but contain locally developed ripple cross-lamination and regular to discontinuous wavy lamination on a millimeter scale (Fig. 5). The lamination is commonly diffuse and poorly defined as a result of disruption by burrowing and bioturbation caused mainly by rootlets up to 10 cm long, which are common throughout the siltstone and claystone.

A feature of the siltstone and claystone is the presence of numerous mottled zones in various shades of brown, yellow, green-

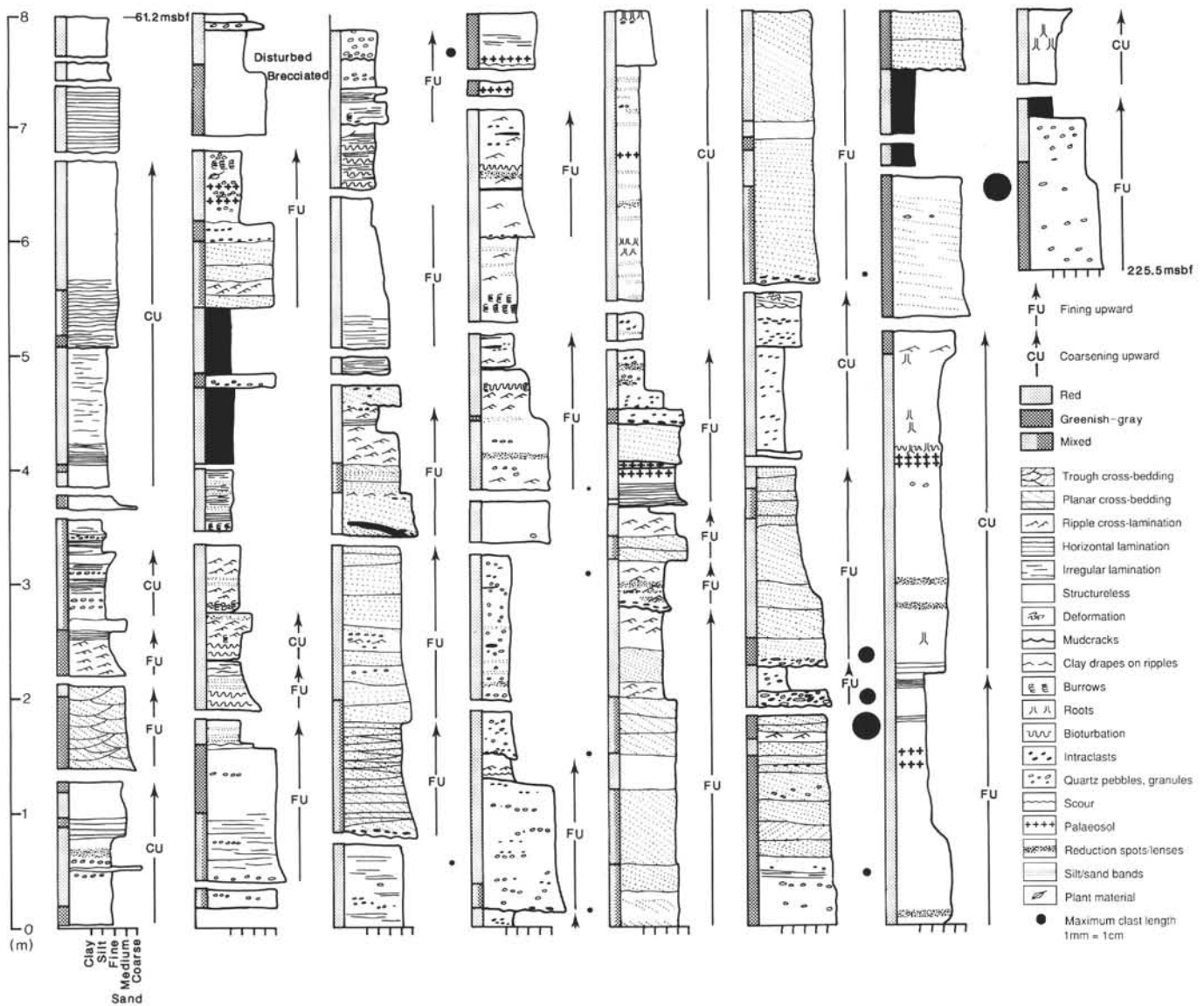


Figure 2. Composite lithologic section of Prydz Bay red beds (Unit III, Hole 740A).

ish gray, and purple. Some mottled siltstones are penetrated by roots and are locally granular and pebbly in character. They contain small, subangular to subrounded pebbles and granules of basement lithology, including granite, gneiss, quartz, feldspar, and metavolcanic rocks. The largest clast measured is some 1.5 cm long. A single example of concave-up mud curls a few millimeters in length, a mud-cracked surface, and convolute lamination (Fig. 2) was also found in the siltstone and claystone.

The coarsening-upward sequences in the succession attain thicknesses of up to 2.3 m, but they are rarely complete owing to poor core recovery. They consist of siltstone and claystone, gradationally or less commonly sharply overlain by fine- to medium-grained sandstone. In some examples fine-grained sandstone and siltstone grade up into coarser grained sandstone at the top. The sandstones at the top of the sequences are mostly structureless, with locally developed ripple cross-lamination, horizontal/irregular lamination, and rare cross-bedding (Fig. 2). The siltstone and claystone are identical to those at the top of the fining-upward sequences.

Interpretation

The erosively based fining-upward sequences in the Prydz Bay core are similar to some of the cyclic sandy braided stream facies profiles of Miall (1977). More detailed comparisons to ancient and modern braided river systems are precluded by the lack of downhole geophysical logs, lateral facies control, and information on sand body geometry. This in turn limits the level of environmental interpretation possible and the extent to which the depositional system can be effectively interpreted (Miall, 1985).

The channel sand bodies were deposited in relatively shallow channels that remained stable for sufficiently long periods of time to allow for the accumulation of significant quantities of flood plain silts and muds from overbank flows and the development of pedogenic processes within the more extensively vegetated distal parts of the overbank environment. Channel stability may have been due to the presence of vegetation, pedogenically cemented overbank alluvium, and topographic relief on

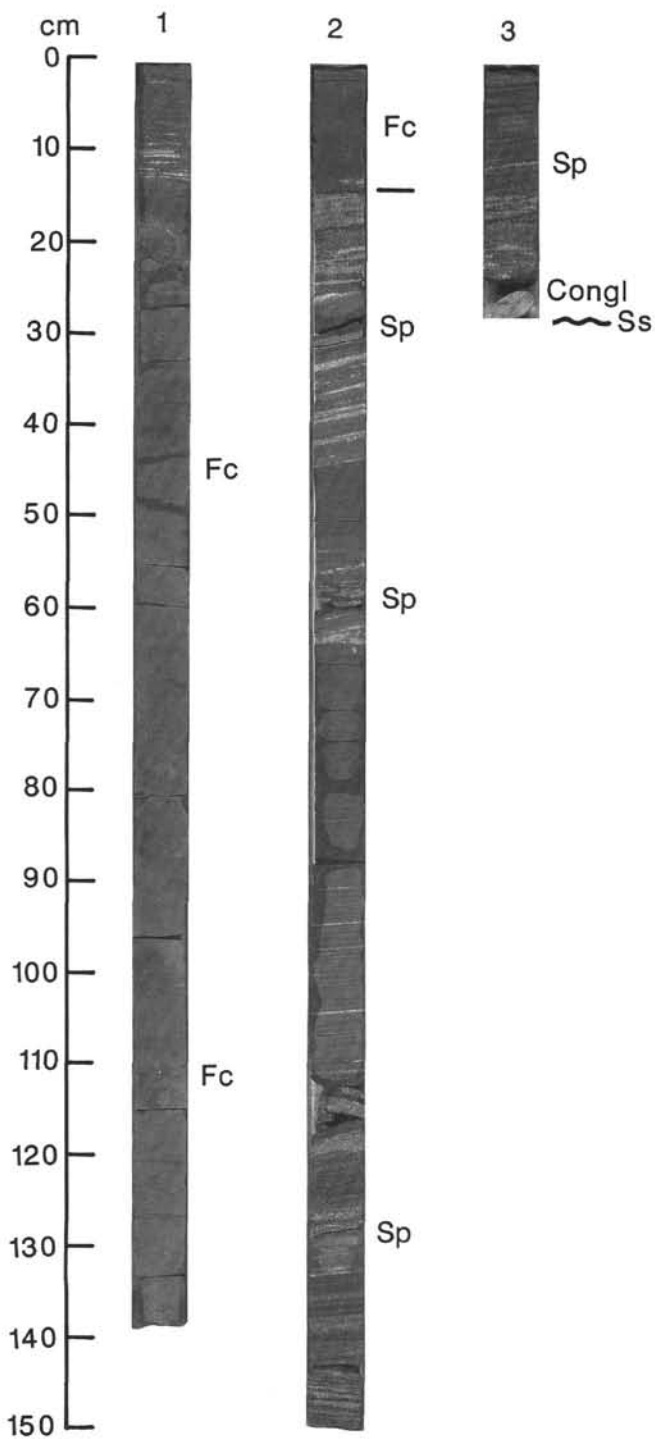


Figure 3. Fining-upward sequence in Core 119-740A-28R consisting of a scoured surface (Ss) and channel lag conglomerate (Congl) overlain by medium- to coarse-grained, low-angle planar cross-bedded sandstone (Sp), which is abruptly overlain by massive and mottled siltstone and silty claystone (Fc). Note the striped red (dark) and pale greenish gray (light) appearance of the planar cross-bedded foresets.

the flood plain, which would have been sufficient to trap fines that would then inhibit channel shifting. This seems to have been most common during deposition of the upper part of the succession. The relatively low incidence of internal scouring and reworking of the channel sand bodies, clay drapes, and other

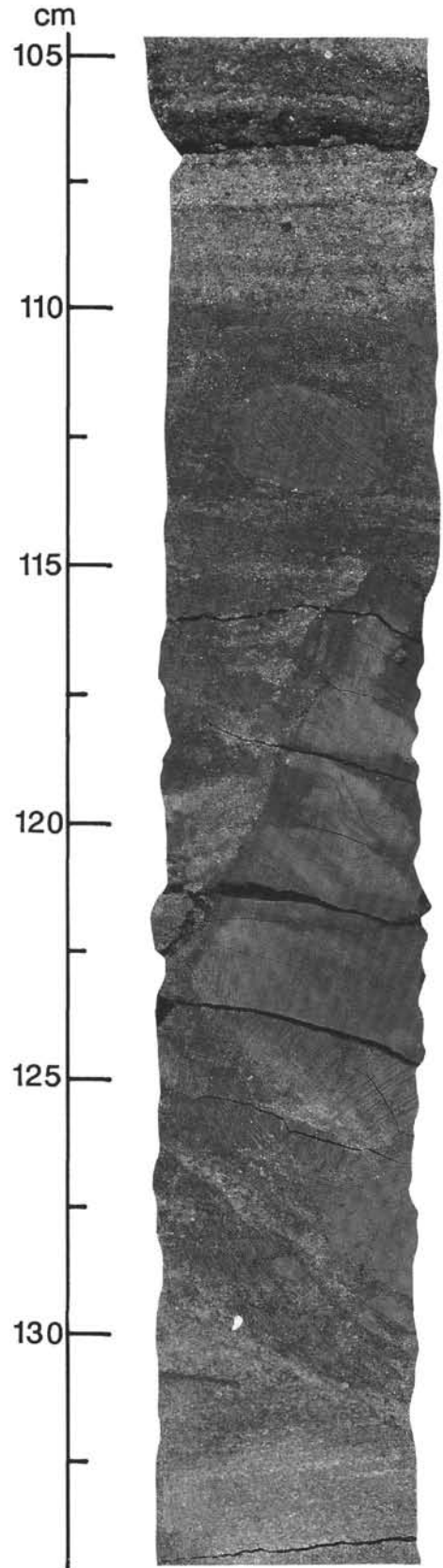


Figure 4. Steep erosion surface with large claystone intraclast interpreted as part of a collapsed channel bank in Section 119-740A-22R-1, 104-134.5 cm. Note the alignment of the smaller, elongate mud clasts parallel to the erosion surface, suggesting downslope movement.

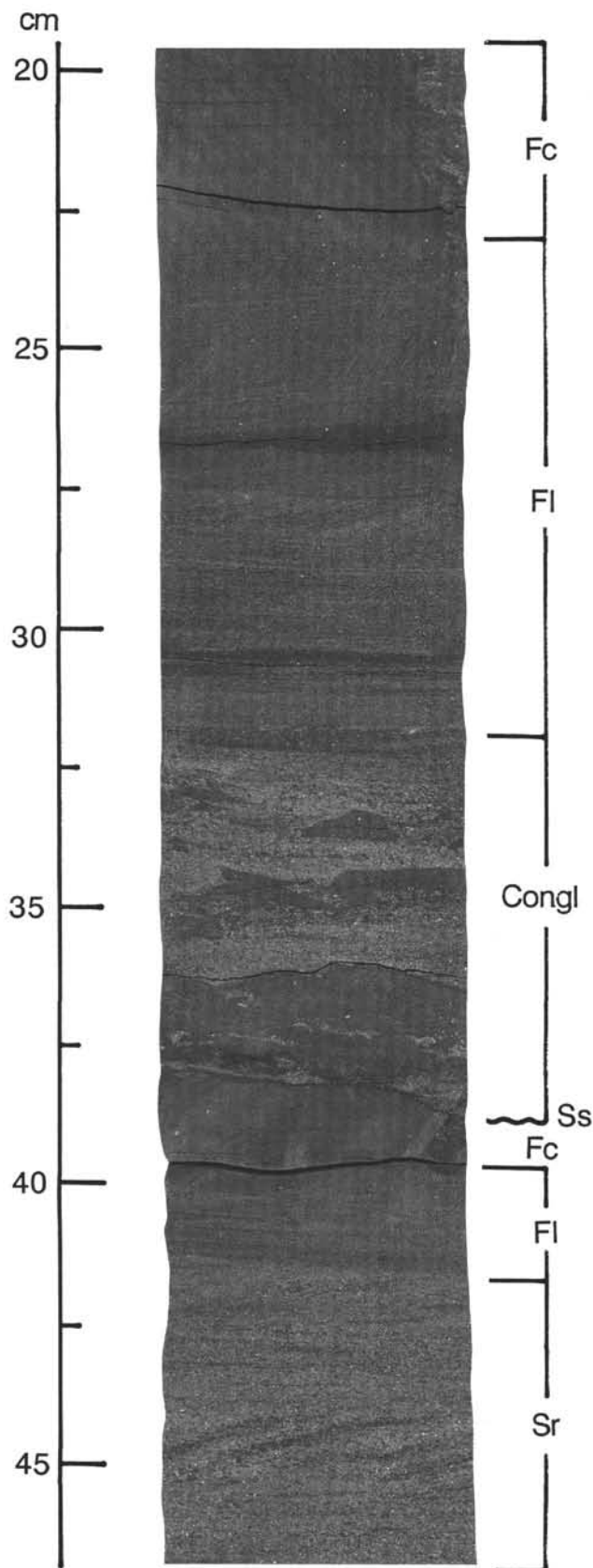


Figure 5. Rippled sandstone (Sr) at top of channel-fill sand body overlain by laminated and rippled overbank siltstone (FI) and massive claystone (Fc) in Section 119-740A-22R-1, 19.5–47 cm. This is succeeded by a fining-upward sequence comprising a scoured surface (Ss), intraformational conglomerate with sandy matrix (Congl), laminated and rippled siltstone (FI), and massive claystone (Fc).

evidence of bedform modification and emergence suggest that discharge fluctuations were not very great during their deposition, in contrast to the more ephemeral systems described by Turner (1978) and Tunbridge (1984), which are characterized by repeated episodes of scour and fill and abundant upper flow regime plane beds. This in turn implies that the climate was sufficiently wet to maintain discharge throughout the channel sand deposition. However, the general fining-upward trend in the channel sand bodies and abrupt change to siltstone and claystone are consistent with the sudden abandonment of most channels through rapid avulsive shifting. The steep erosion surface in Figure 4 is interpreted as a channel bank cut into coherent mud and silt, which afforded considerable resistance to erosion. The resistant nature of the channel banks would also have facilitated abrupt avulsive events.

The dominance of planar cross-bedding suggests that the channels may have been occupied mainly by simple transverse bars or two-dimensional dune bedforms with only limited development of in-channel three-dimensional dune (trough) bedforms. However, the lack of lateral control on the nature of the cross-bedding makes identification of the original bedforms uncertain. Although local changes in hydrodynamic conditions enabled ripples to form, there is no evidence to suggest the extensive development of bar-top bedforms consistent with rapidly fluctuating flows. The flume experiments of Jopling (1965) show that nonerosive basal contacts and low-angle foresets are a result of relatively weak flow velocities characterized by a low ratio of suspension load to bedload. Very little of the suspension load was deposited on the slip face, which was dominated by grain avalanching. The constant shape and dip of the foresets and absence of reactivation surfaces imply deposition under steady-state flow conditions, at water depths sufficiently high to allow for the deposition of cosets. The difference in color of the channel sand bodies probably reflects fluctuations in the level of the water table during deposition. Thus, the greenish gray drab sandstones remained mostly below the water table, where reducing conditions prevailed, particularly in the presence of organic matter (Turner, 1980). Any oxides or hydroxides unstable under these conditions would be removed. Where the sandstones remained above the water table under more oxidizing conditions, the iron oxides and hydroxides, which are mainly contained within the clay minerals, imparted a red color to the sediment. Local reduction spots and lenses in these red oxidized sandstones are mainly linked to decaying organic matter. On oxidation, this releases CO_2 , which is a powerful reducing agent. The regular alternation of red and green texturally graded foreset laminae suggests that the critical factor here was differences in grain size controlled primarily by hydrodynamic sorting processes during avalanching down the lee face of the original bedform (Allen, 1983). The coarser bedload-dominated drab-colored laminae are more porous and permeable than the finer grained, clay-rich red laminae, with the result that reducing groundwaters were able to concentrate along this local permeable/impermeable boundary.

The siltstones and claystones represent fine-grained flood plain deposits laid down during inundation and flooding of the overbank environments. Floodwaters carried mainly silt and mud, with coarser sand deposited during major flood events. Most of the coarser silt and sand in the overbank fines occurs as thin diffuse layers and lenses rather than discrete beds with sharp bases and tops. The diffuse graded nature of some of the laminae is consistent with sediment fallout from suspension, as described by De Raaf et al. (1977). Similar laminations have also been attributed to weak, dilute density flows (Collinson and Thompson, 1982). The nature of the silt and sand layers implies that the floods were small, low-energy, short-lived events and that the overbank environment may have been waterlogged

at the time of flood incursion; hence, the scarcity of mud cracks in the flood plain deposits and the paucity of sharp bedding contacts. The scarcity of mud cracks further suggests that the overbank environment was waterlogged between flood episodes. This interpretation is consistent with the lack of pedogenic carbonate, which generally requires an arid to semiarid seasonal climate with a low rainfall for its formation, as discussed in the following section. The inability of the depositional surface to dry out completely between flood events may reflect the high silt content of the flood plain deposits. Under these conditions, the randomly distributed siltstone and claystone intraclasts in the floodplain deposits may have been derived from within the channel or the floodplain during flood events, with their small size reflecting the competence of the flow in the upper part of the water column in the channel. Each fining-upward sequence within the overbank deposits records a single episode of flooding and overbank deposition under decelerating flow conditions.

Most of the overbank siltstones and claystones lack sedimentary structures. This lack of structure in the core and in thin section, together with the presence of abundant rootlets (indicative of emergence and colonization by plants), burrows, bioturbation, and extensive color mottling is attributed to pedogenic processes. Additional micromorphological evidence of pedogenesis is the presence of voids, ped structures, and plasmic fabrics (B. R. Turner, unpubl. data) typical of modern soils seen in thin section. In contrast to many pedogenically influenced red beds, the sediments contain no pedogenic carbonate other than a micritic root structure in Sample 119-740A-26R-4, 6–10 cm. Pedogenic carbonate (calcrete) normally requires a prolonged period of dryness (seasonal climate) for its formation, irrespective of its climatic setting. However, extensive calcrete formation is favored by arid to semiarid climatic conditions, low rainfall, and negligible sediment input into the area for prolonged periods of time (Allen, 1974; Leeder, 1975). Thus, the lack of carbonate in the sediments could be due to climatic factors (climate too wet or rainfall not seasonally peaked enough), high sedimentation rates, the presence or absence of carbonate in the source rocks, and acid waters that remove carbonate in solution. The relative importance of these factors is difficult to assess, but the inferred fluctuations in the water table and perennial nature of the channels suggest that the climate may have been too wet for extensive pedogenic carbonate formation (Bown and Krause, 1981). Although the 500-mm isohyet is generally taken as the upper limit for calcrete formation, incipient calcrete has been known to form in environments with up to 1500 mm of annual precipitation (Reeves, 1970).

The gradational coarsening-upward sequences in the succession are interpreted to have resulted from local increases in flow intensity and sediment concentration due to flooding of the lower-lying overbank environment. More rapid flooding by sand-laden currents, and the local development of crevasse channels or splay lobes, may have been responsible for the sharply based sandstone at the top of one coarsening-upward sequence (Elliott, 1974). Any abandonment facies that might have been present above this sandstone are not seen because of core loss.

PETROGRAPHY

Description

Modal analysis of sandstones and siltstones (Table 1) in the succession, based on a count of 300 grains per slide, shows that compositionally they are predominantly poorly sorted, immature sediments containing more than 17% clay matrix. The sandstones are arkosic wackes (Fig. 6 and Pl. 1, Fig. 1) composed of quartz, mica, and feldspar with subordinate rock fragments, garnet, and opaque minerals set in a clay matrix that makes up

between 17% and 66% of the rock (Table 1). Chlorite and sericite are common constituents of the matrix, some of which is diagenetic. In some sections the matrix consists predominantly of a coarse mat of biotite, muscovite, sericite, and chlorite, with individual grains up to 0.024 mm in length, or medium silt grade. The matrix also includes rare authigenic vermicular crystals of chlorite. Other coarse chlorite grains without any obvious mineral precursors may be detrital in origin. X-ray-diffraction analysis shows that in addition to chlorite and sericite the matrix includes illite-smectite and kaolinite. Fine shreds of mica and clay minerals coat the surface of many detrital quartz and feldspar grains. The quartz grains in the coarser grained channel sandstones (Table 1) attain lengths of up to 1.2 mm. The relationship between percentage detrital quartz and grain size for different fluvial environments is shown in Figure 7. The relationship serves to differentiate between channel and overbank deposits depicted in Table 1, with a further more refined subdivision into proximal and distal overbank deposits. Splay deposits are not common and lie close to the boundary between channel and overbank deposits. The quartz grains are mostly subangular, but range from angular to subrounded types, with rare, well-rounded second-cycle grains (Pl. 1, Fig. 2). In the more clay-rich sandstones the quartz and other detrital grains "float" in the clay matrix, which is red and impregnated with iron oxides (mainly hematite) or less commonly greenish gray and rich in chlorite. Some of the quartz grains show poorly developed secondary overgrowths defined by a thin rim of dust and iron oxide. A feature of many of the grains is the presence of inclusions, particularly needles of sillimanite (Pl. 1, Fig. 3).

The feldspars are predominantly orthoclase with minor amounts of microcline and perthite. Plagioclase is absent or present in amounts of 1% or less. Feldspar abundance is orthoclase > microcline > perthite > plagioclase. The orthoclase occurs as relatively fresh to slightly altered angular, prismatic grains, up to 0.6 mm long, some of which show exsolution features. Sporadic iron-staining occurs along cleavage planes, and in a few cases grains contain inclusions of other minerals, some with alignment parallel to the long axis of the feldspar. The feldspars are commonly larger in size than the quartz grains.

Biotite is the dominant mica in most sandstones, and in some cases it may make up as much as 38% of the rock. It occurs as large, elongate detrital grains and shredlike flakes, up to 0.4 mm long, some of which are bent and folded around other detrital grains through intergranular pressure. The more elongate grains tend to have their long axes aligned parallel to one another, thereby imparting a distinct fabric to the sandstone, especially the finer grained varieties. The biotite grains are relatively fresh or show various stages of alteration, principally to hematite. Completely altered grains, however, are rare. Muscovite occurs as small shredlike flakes, usually associated with chlorite, or less commonly as large detrital grains.

Rock fragments are present in most of the sandstones, but are not very common and never exceed 6% of the rock. They consist mainly of (1) rounded fragments of granite/gneiss composed of quartz + muscovite + chlorite + feldspar up to 0.7 mm long (Pl. 1, Fig. 4); (2) coarse chlorite aggregates, which represent alteration of an earlier mineral phase that has rounded outlines still discernible; and (3) more angular polycrystalline quartz grains that are generally smaller than the chloritic rock fragments (maximum 0.48 to 0.56 mm long) (Pl. 1, Fig. 4). Most of the chloritized grains appear to have undergone alteration prior to burial and diagenesis. Some of the quartz grains are characterized by stretched, elongate crystals with crenulated margins typical of a metamorphic source. Others are more typical of an igneous derivation in that they comprise crystals showing a large variation in crystal size. Needlelike inclusions (?sillimanite) are distributed throughout a few of the polycrystalline

Table 1. Mineral composition of sandstones and siltstones from Hole 740A.

| Core, section, interval (cm) | Lithology | Dominant Color | Mean grain size | Environment | Quartz | Orthoclase | Feldspars Microcline | Plagioclase | Rock fragments | Biotite | Muscovite | Clay matrix | Opaque minerals |
|------------------------------|-----------------|----------------|-----------------|-------------|--------|------------|----------------------|-------------|----------------|---------|-----------|-------------|-----------------|
| a 8R-CC, 15-17 | Sandstone | 10YR 6/1 | 1.55 | Channel | 31 | 14 | 2 | T | 1 | | | 39 | 9 |
| 12R-1, 29-32 | Sandstone | 7.5YR 2/1 | 2.06 | Splay | 39 | 11 | T | T | 1 | 4 | 1 | 37 | 6 |
| 12R-1, 41-45 | Sandstone | 5Y 5/1 | 2.47 | Splay | 33 | 8 | | | | 5 | 7 | 40 | 6 |
| 12R-1, 55-58 | Sandstone | 7.5YR 2/1 | 3.68 | Overbank | 17 | 4 | T | | 2 | 6 | | 66 | 5 |
| 14R-1, 34-36 | Siltstone | 10R 3/2 | 3.98 | Overbank | 11 | 2 | 1 | | 1 | 10 | 1 | 69 | 5 |
| a 14R-1, 99-102 | Sandstone | 10R 2.5/1 | 1.58 | Channel | 27 | 7 | | | 3 | | T | 54 | 5 |
| | | 10R 4/2 | | | | | | | | | | | |
| 14R-2, 41-43 | Sandstone | 5G 6/1 | 1.97 | Channel | 27 | 4 | 2 | | 2 | | | 62 | 2 |
| 15R-1, 32-34 | Sandstone | 10R 3/2 | 3.06 | Overbank | 26 | 1 | | | 1 | 20 | 4 | 43 | 4 |
| 17R-1, 100-103 | Sandstone | 10R 5/2 | 1.95 | Channel | 29 | 6 | 2 | | 4 | T | 1 | 50 | 5 |
| | | 5G 4/2 | | | | | | | | | | | |
| 19R-1, 10-14 | Sandstone | 5YR 3/1 | 3.18 | Overbank | 24 | 5 | T | | | 24 | 4 | 41 | 2 |
| 19R-1, 35-38 | Siltstone | 5YR 3/2 | 4.51 | Overbank | 11 | | | | | 3 | 2 | 81 | 3 |
| 19R-1, 47-48 | Sandstone | 5YR 3/2 | 2.74 | Overbank | 31 | 10 | T | | | 7 | 3 | 38 | 9 |
| 19R-1, 63-65 | Sandstone | 5YR 3/2 | 2.63 | Overbank | 30 | 11 | T | | 1 | 12 | | 44 | 2 |
| 19R-1, 77-79 | Sandstone | 5YR 3/2 | 3.7 | Overbank | 35 | 2 | | | | 38 | 7 | 17 | 1 |
| 19R-1, 85-88 | Siltstone | 5YR 3/2 | 4.76 | Overbank | 14 | 1 | | | | 1 | T | 83 | 1 |
| 20R-3, 73-75 | Siltstone | 5YR 3/2 | 5.01 | Overbank | 10 | T | | | T | 2 | | 87 | 1 |
| 20R-3, 119-121 | Silty sandstone | 5YR 3/2 | 3.84 | Overbank | 21 | 2 | 1 | 1 | 1 | 10 | T | 60 | 4 |
| 20R-4, 42-44 | Sandstone | 5YR 3/2 | 2.55 | Overbank | 25 | 8 | T | T | 2 | 16 | 1 | 44 | 3 |
| 22R-1, 8-10 | Sandstone | 5YR 8/1 | 2.24 | Channel | 39 | 7 | T | T | 6 | 2 | 1 | 39 | 4 |
| | | 5YR 3/2 | | | | | | | | | | | |
| 22R-2, 85-87 | Sandstone | 5YR 5/1 | 1.44 | Channel | 30 | 11 | 2 | 1 | 2 | 6 | T | 45 | 3 |
| | | 5YR 4/2 | | | | | | | | | | | |
| 23R-1, 102-108 | Sandstone | 5GY 5/1 | 3.97 | Overbank | 13 | 3 | | | 2 | 23 | 1 | 55 | 3 |
| 23R-1, 106-108 | Sandstone | 5Y 2.5/1 | 2.82 | Overbank | 27 | 11 | | | | 11 | 11 | 44 | |
| 24R-1, 103-106 | Sandstone | 5YR 3/2 | 2.51 | Channel | 34 | 8 | T | T | 1 | 8 | | 45 | 2 |
| 25R-1, 16-18 | Siltstone | 10R 4/4 | 2.91 | Overbank | 24 | 3 | T | | T | 12 | 2 | 57 | 2 |
| 25R-1, 99-101 | Sandstone | 10G 6/1 | 1.88 | Channel | 23 | 12 | 3 | | 3 | 10 | T | 47 | 2 |
| 26R-2, 136-139 | Sandstone | 10R 4/2 | 1.2 | Channel | 40 | 19 | 1 | | 2 | 3 | T | 32 | 2 |
| 26R-3, 20-24 | Sandstone | 10R 3/3 | 3.88 | Overbank | 14 | 4 | T | | T | 13 | 1 | 66 | 3 |
| b 26R-4, 6-10 | Sandstone | 2.5Y 8/1 | 3.53 | Overbank | 13 | 4 | | | | | 2 | 80 | 1 |
| | | 2.5 YR 3/4 | | | | | | | | | | | |
| 26R-4, 7-10 | Sandstone | 2.5 Y 8/1 | 2.69 | Overbank | 17 | 10 | T | | 2 | 5 | T | 60 | 3 |
| 26R-4, 48-51 | Sandstone | 2.5YR 2.5/4 | 3.32 | Overbank | 22 | 11 | T | | | 7 | 1 | 55 | 2 |
| 27R-4, 9-12 | Sandstone | 10R 3/1 | 2.16 | Channel | 30 | 4 | T | | 2 | 4 | T | 46 | 10 |
| 27R-5, 19-21 | Sandstone | 10R 3/2 | 1.76 | Channel | 33 | 14 | T | | 4 | 4 | T | 44 | 1 |
| 27R-5, 135-138 | Sandstone | 10R 3/2 | 1.81 | Channel | 21 | 5 | | 1 | T | 5 | 4 | 64 | |
| 28R-3, 31-34 | Silty sandstone | 10R 3/3 | 4.06 | Overbank | 15 | 5 | | | 1 | 11 | | 59 | 9 |
| 30R-1, 4-5 | Sandstone | 7.5G 3/2 | 2.49 | Channel | 21 | 4 | | T | | 3 | 1 | 69 | 2 |
| | | 10G 4/2 | | | | | | | | | | | |
| 31R-1, 89-92 | Sandstone | 10R 2.5/1 | 2.88 | Overbank | 27 | 4 | | | | 9 | 1 | 54 | 4 |
| | | 5GY 5/1 | | | | | | | | | | | |
| 31R-3, 4-8 | Sandstone | 5YR 3/2 | 4.35 | Overbank | 16 | 4 | | | | 6 | 8 | 64 | 2 |
| 31R-5, 25-28 | Sandstone | 5YR 3/2 | 0.76 | Channel | 33 | 20 | | | T | | 1 | 44 | 2 |

a Contains traces of clinopyroxene and olivine

b Calcareous root structure

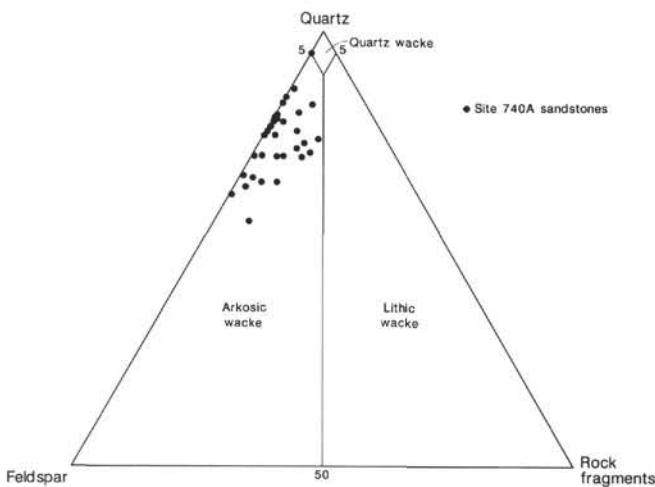


Figure 6. Classification of Prydz Bay sandstones (after Pettijohn et al., 1987). The sandstones contain more than 17% clay matrix.

quartz grains. Other lithologic types, which occur as rock fragments, include claystone, siltstone, and quartz-mica schist.

Garnet is present in most sandstones, particularly the coarser varieties where it may make up as much as 4% of the rock. Garnet occurs as fresh, angular to subrounded grains (Pl. 1, Fig. 5),

ranging from 0.03 to 0.42 mm in size. The garnet grains are predominantly colorless to pale pink in thin section but include some green varieties, especially in Sample 119-740A-22R-1, 8-10 cm. Microprobe analysis of individual garnet grains shows them all to be iron-rich almandine garnets, containing relatively little manganese (0.89%–7.16%), magnesium (2.34%–7.77%), and calcium (3.38%–5.52%) (Fig. 8). The opaque mineral suite includes magnetite, pyrite, hematite, ilmenite, and titaniferous-rich magnetite. Spinel was also identified during routine shipboard analysis of smear slides. Rare clinopyroxenes and one olivine crystal were found in two greenish gray, reduced, chlorite-rich sandstones containing abundant ilmenite and titanomagnetite. These sandstones (Samples 119-740A-8R-CC, 15-17 cm, and 119-740A-14R-1, 99-102 cm) have anomalously high TiO₂ and MnO contents (Table 2). The ilmenite and titanomagnetite tend to concentrate into laminae rich in dark, heavy minerals (Pl. 1, Fig. 6), associated with abundant garnets in one of the sandstones. In addition to garnet, ilmenite, and magnetite, the heavy mineral suite in the sandstones includes tourmaline, hematite, and pyrite.

Interpretation

The composition of the sandstones (arkosic wackes), their immaturity, and the angularity of the detrital grains are consistent with a provenance of high relief undergoing rapid erosion, with the resulting detritus transported and deposited quickly. This in turn implies a provenance in close proximity to the depo-

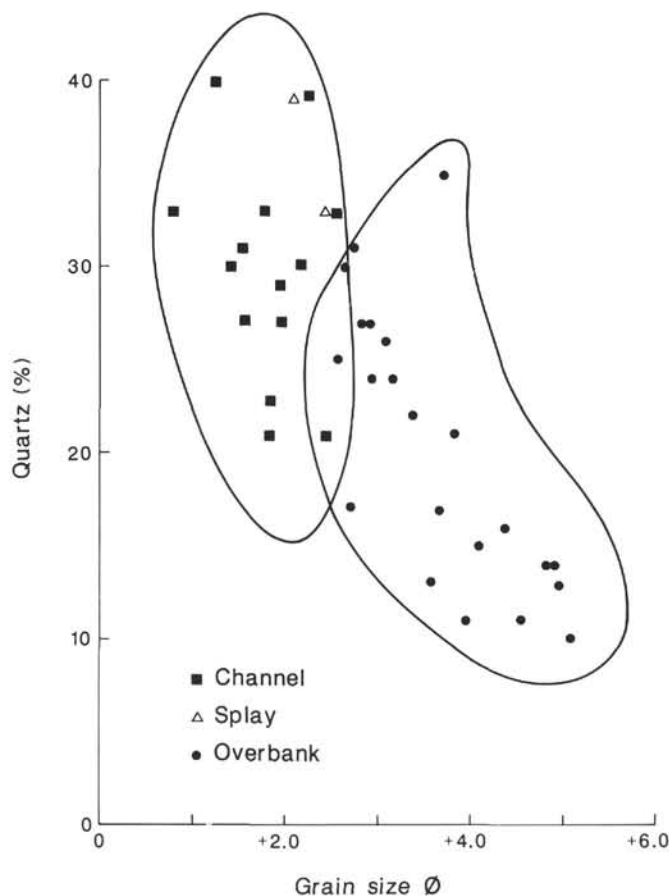


Figure 7. Percentage detrital quartz against grain size for different fluvial environments. The coarser grained overbank deposits with a higher percentage of quartz represent more proximal overbank deposits. Data from Table 1.

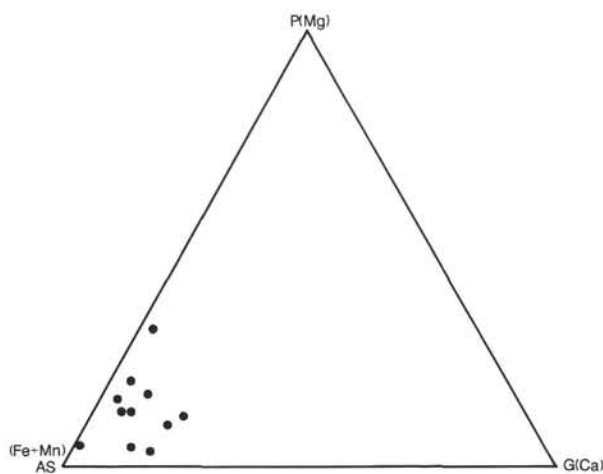


Figure 8. Composition of detrital garnet grains from Prydz Bay red beds, Hole 740A. P = pyrope; AS = almandine + spessartine; G = grossular.

sitional site that underwent rapid uplift. The rate of uplift and erosion may have exceeded the rate of weathering in the source area, as evidenced by the abundance of relatively fresh biotite and orthoclase in the sandstone. This view is strengthened by the locally preserved clinopyroxene and olivine in two of the sandstone samples, as these are normally the first minerals to be destroyed prior to burial. Thus, whilst the rate of uplift and erosion was sufficient to prevent excessive weathering and loss of biotite and orthoclase, it was not rapid enough to preserve most of the less stable minerals, such as pyroxene and olivine. Estimates of the rate of erosion and source area relief are precluded by the poor core recovery and lack of paleontological control. However, such rapid uplift implies a tectonic control, possibly related to rifting associated with the development of the Lambert Graben prior to continental breakup. Support for a tectonically active source comes from the work of Folk (1968), who suggested that the presence of angular quartz and feldspar in a sediment, in which feldspar is relatively fresh and commonly larger than the quartz grains, is tectonically derived. He referred to such sandstones as "tectonic arkoses" and considered them to form mainly as alluvial fans or piedmonts, along the margins of block-faulted, usually granitic, mountainous terrains (Folk, 1968, p. 132).

Provenance uplift may in turn have influenced climate at the source and the rate of basin subsidence thought to have been responsible for the fining-upward trend shown by the succession. Once deposition and burial had occurred, early diagenetic alteration and dissolution appear to have been limited, as witnessed by the relatively fresh nature of most detrital grains, particularly the more unstable biotite and orthoclase grains. This may be the reason for the lack of authigenic silica in the sediments, for which the source normally is the alteration and/or replacement of the labile silicates at shallow depths in most red bed successions (Turner, 1980). Similarly, the lack of carbonate inhibits conditions suitable for the pore-water dissolution of silica generated in this way, and as a result, secondary quartz overgrowths are poorly developed.

The mineralogy of the sandstones indicates that they were derived from a high-grade metamorphic terrain. Detritus from this terrain must have been diluted with second-cycle material of metasedimentary origin that probably formed part of the same provenance. The detrital mineralogy of the sandstones and the *in-situ* clasts suggest that the gneisses were predominantly of granitic composition but with contributions from a more mafic provenance rock component, as evidenced by the presence of rarely preserved clinopyroxene and olivine (Table 1), the high Cr and Ni content of the sediments (Table 2), and the presence of titaniferous rich magnetite. The importance of the mafic provenance is difficult to assess from the mineralogy because mafic and ultramafic components are much less likely to be preserved in a sediment than granite. Nevertheless, the abundance of orthoclase feldspar with virtually no plagioclase is typical of granitic source rocks, especially those within a cratonic setting. Although seismic data reveal the presence of basement ridges within Prydz Bay (Stagg, 1985), the only nearby rocks of this general composition are the upper Proterozoic granulite facies gneisses of the Prydz Bay coast and the Archaean granulite facies of the Vestfold cratonic block (Fig. 1). The relative importance of these two potential sources is uncertain in the absence of paleocurrent data and regional facies patterns. Also, the section of core examined represents only a small part (65 m) of a prebreakup sequence more than 2 km thick (Stagg, 1985).

DISCUSSION

The succession shows an overall fining-upward trend, as reflected in the ratio of sandstone to siltstone and claystone. This

Table 2. Chemical composition of sediments from Hole 740A.

| Core, section, sample interval (cm) | Lithology | SiO ₂ (%) | Al ₂ O ₃ (%) | Fe ₂ O ₃ (%) | MgO (%) | CaO (%) | Na ₂ O (%) | K ₂ O (%) | Ignition loss at 750°C for 3 hr | TiO ₂ (%) | MnO (%) | P ₂ O ₅ (%) | Cr (ppm) | Li (ppm) | Ni (ppm) | Co (ppm) | Zn (ppm) | Cu (ppm) | Total |
|---|-------------------------|-------------------------|---------------------------------------|---------------------------------------|------------|------------|--------------------------|-------------------------|---------------------------------------|-------------------------|------------|--------------------------------------|-------------|-------------|-------------|-------------|-------------|-------------|-------|
| 8R-CC, 15-17 | Sandstone | 65.5 | 12.4 | 8.47 | 1.99 | 0.81 | 0.85 | 1.61 | 3.00 | 2.35 | 0.39 | 0.07 | 220 | 6 | 30 | 33 | 57 | 26 | 97.5 |
| 12R-1, 29-21 | Sandstone | 67.8 | 13.1 | 7.47 | 1.41 | 0.56 | 0.77 | 2.52 | 3.74 | 0.88 | 0.06 | 0.04 | 140 | 12 | 38 | 17 | 53 | 18 | 98.3 |
| 12R-1, 55-58 | Sandstone | 61.3 | 17.0 | 9.18 | 2.03 | 0.56 | 0.85 | 2.52 | 5.00 | 0.82 | 0.05 | 0.03 | 140 | 22 | 79 | 20 | 81 | 45 | 99.4 |
| 13R-1, 37-39 | Sandstone | 51.7 | 14.6 | 19.3 | 1.57 | 0.44 | 0.66 | 2.31 | 5.64 | 0.82 | 0.11 | 0.12 | 180 | 21 | 86 | 34 | 86 | 45 | 97.3 |
| 14R-1, 34-36 | Siltstone | 60.0 | 16.2 | 12.0 | 1.97 | 0.50 | 0.64 | 2.25 | 5.33 | 0.84 | 0.09 | 0.08 | 156 | 22 | 87 | 33 | 87 | 61 | 99.95 |
| 14R-1, 99-102 | Sandstone | 67.4 | 13.3 | 7.07 | 1.78 | 0.92 | 0.88 | 1.26 | 3.42 | 3.08 | 0.52 | 0.11 | 185 | 6 | 28 | 24 | 48 | 14 | 99.77 |
| 14R-2, 41-43 | Sandstone | 52.0 | 20.3 | 11.0 | 2.40 | 0.73 | 0.93 | 2.38 | 5.60 | 0.90 | 0.09 | 0.06 | 220 | 32 | 71 | 30 | 114 | 60 | 96.5 |
| 15R-1, 32-34 | Siltstone | 61.4 | 15.4 | 8.87 | 2.34 | 0.69 | 0.73 | 2.38 | 4.73 | 0.85 | 0.19 | 0.09 | 140 | 23 | 63 | 26 | 82 | 26 | 97.7 |
| 15R-1, 137-140 | Siltstone | 57.9 | 17.6 | 10.6 | 2.44 | 0.56 | 0.74 | 2.38 | 5.12 | 0.72 | 0.20 | 0.11 | 151 | 30 | 80 | 30 | 98 | 46 | 98.41 |
| 17R-1, 100-103 | Sandstone | 78.9 | 11.1 | 2.10 | 0.96 | 0.54 | 0.68 | 3.07 | 2.59 | 0.16 | 0.02 | 0.04 | 59 | 7 | 15 | 6 | 24 | 9 | 100.2 |
| 19R-1, 63-65 | Siltstone | 66.1 | 15.3 | 6.25 | 1.55 | 0.86 | 0.90 | 3.15 | 4.25 | 0.54 | 0.04 | 0.15 | 98 | 16 | 52 | 22 | 53 | 53 | 99.1 |
| 19R-1, 85-88 | Siltstone | 51.3 | 19.1 | 14.51 | 1.95 | 0.52 | 0.58 | 2.35 | 6.84 | 0.88 | 0.10 | 0.10 | 200 | 43 | 85 | 34 | 106 | 71 | 98.3 |
| 20R-3, 73-75 | Siltstone | 51.0 | 21.8 | 10.4 | 2.17 | 0.56 | 0.58 | 2.39 | 7.13 | 0.90 | 0.07 | 0.07 | 240 | 50 | 94 | 34 | 109 | 66 | 97.1 |
| 20R-3, 119-121 | Sandstone | 51.2 | 17.5 | 17.8 | 1.88 | 0.61 | 0.75 | 2.46 | 6.44 | 0.83 | 0.12 | 0.15 | 119 | 32 | 81 | 29 | 104 | 72 | 99.8 |
| 20R-4, 42-44 | Sandstone | 65.1 | 15.6 | 6.65 | 1.75 | 0.74 | 0.70 | 2.75 | 4.51 | 0.83 | 0.06 | 0.05 | 124 | 19 | 56 | 17 | 77 | 32 | 98.8 |
| 22R-1, 8-10 | Sandstone | 77.5 | 11.4 | 2.58 | 1.04 | 0.62 | 0.70 | 2.68 | 2.84 | 0.39 | 0.04 | 0.03 | 62 | 7 | 21 | 7 | 31 | 22 | 99.8 |
| 22R-2, 85-87 | Sandstone | 68.5 | 15.1 | 4.89 | 1.28 | 0.64 | 0.88 | 3.57 | 4.34 | 0.50 | 0.05 | 0.03 | 99 | 17 | 58 | 13 | 68 | 38 | 99.8 |
| 23R-1, 52-55 | Sandstone | 60.2 | 16.8 | 9.28 | 2.44 | 1.04 | 0.78 | 2.55 | 5.75 | 0.76 | 0.07 | 0.06 | 160 | 22 | 112 | 54 | 112 | 41 | 99.8 |
| 23R-1, 102-106 | Sandstone | 66.3 | 13.8 | 8.18 | 1.66 | 0.70 | 0.72 | 2.71 | 4.21 | 0.71 | 0.06 | 0.04 | 120 | 15 | 37 | 16 | 74 | 32 | 99.1 |
| 24R-1, 103-106 | Sandstone | 66.3 | 14.4 | 6.90 | 1.75 | 0.97 | 0.87 | 2.54 | 4.49 | 0.82 | 0.08 | 0.10 | 124 | 13 | 54 | 24 | 61 | 33 | 99.3 |
| 25R-1, 16-18 | Siltstone | 62.0 | 16.1 | 8.94 | 1.99 | 0.72 | 0.60 | 2.33 | 4.97 | 0.86 | 0.08 | 0.08 | 146 | 23 | 70 | 29 | 82 | 56 | 98.71 |
| 25R-1, 99-101 | Sandstone | 70.7 | 12.9 | 6.00 | 1.15 | 0.54 | 0.54 | 2.82 | 3.69 | 0.51 | 0.08 | 0.06 | 66 | 17 | 46 | 20 | 58 | 21 | 99.0 |
| 26R-2, 136-139 | Sandstone | 73.5 | 12.7 | 4.10 | 0.98 | 0.68 | 0.66 | 3.33 | 3.29 | 0.61 | 0.06 | 0.05 | 67 | 8 | 27 | 12 | 41 | 8 | 100.0 |
| 26R-3, 20-24 | Sandstone | 72.4 | 12.9 | 4.41 | 1.51 | 0.85 | 0.68 | 2.60 | 3.46 | 1.04 | 0.16 | 0.08 | 144 | 14 | 48 | 45 | 140 | 218 | 100.2 |
| 26R-4, 6-10 | Sandstone | 61.0 | 17.4 | 9.10 | 2.36 | 0.88 | 0.72 | 2.64 | 5.50 | 0.72 | 0.11 | 0.05 | 124 | 23 | 65 | 24 | 85 | 56 | 100.5 |
| 26R-4, 48-51 | Silty claystone | 60.9 | 16.9 | 8.58 | 2.28 | 0.74 | 0.62 | 2.65 | 4.46 | 0.81 | 0.09 | 0.06 | 146 | 22 | 80 | 27 | 75 | 55 | 98.13 |
| 27R-1, 107-111 | Sandstone | 54.7 | 22.1 | 9.67 | 2.04 | 0.80 | 0.64 | 2.66 | 6.69 | 0.77 | 0.07 | 0.04 | 172 | 34 | 60 | 22 | 109 | 37 | 100.2 |
| 27R-1, 134-136 | Sandstone | 55.8 | 18.7 | 11.1 | 2.26 | 0.81 | 0.64 | 2.26 | 6.20 | 0.88 | 0.12 | 0.09 | 132 | 30 | 94 | 43 | 110 | 37 | 98.9 |
| 27R-4, 9-12 | Sandstone | 67.6 | 13.0 | 7.39 | 1.55 | 0.97 | 0.71 | 1.89 | 4.32 | 1.32 | 0.13 | 0.09 | 160 | 8 | 35 | 16 | 65 | 11 | 99.0 |
| 27R-5, 19-21 | Sandstone | 75.0 | 12.5 | 2.93 | 1.24 | 0.80 | 0.68 | 2.67 | 3.47 | 0.33 | 0.03 | 0.04 | 80 | 7 | 29 | 12 | 39 | 12 | 99.7 |
| 28R-1, 43-47 | Silty claystone | 53.8 | 21.4 | 11.0 | 2.38 | 0.98 | 0.52 | 2.22 | 7.05 | 0.77 | 0.09 | 0.11 | 160 | 41 | 115 | 40 | 111 | 47 | 100.4 |
| 28R-1, 133-137 | Siltstone | 61.4 | 16.5 | 9.44 | 2.26 | 0.88 | 0.64 | 2.52 | 5.41 | 0.84 | 0.08 | 0.12 | 218 | 22 | 85 | 30 | 86 | 81 | 100.1 |
| 28R-3, 31-34 | Siltstone | 53.0 | 20.4 | 12.3 | 2.40 | 0.82 | 0.48 | 2.26 | 6.73 | 0.75 | 0.09 | 0.16 | 156 | 39 | 113 | 34 | 115 | 53 | 99.4 |
| 31R-1, 89-92 | Sandstone | 59.0 | 15.4 | 11.6 | 1.72 | 0.60 | 0.48 | 2.26 | 5.09 | 0.88 | 0.08 | 0.06 | 197 | 19 | 65 | 24 | 83 | 37 | 97.21 |
| 31R-3, 8-11 | Claystone/ Sandstone | 52.2 | 18.7 | 14.7 | 2.31 | 1.03 | 0.68 | 1.91 | 7.14 | 0.66 | 0.10 | 0.08 | 780 | 27 | 110 | 35 | 120 | 33 | 99.6 |
| 31R-4, 108-111 | Silty claystone | 53.0 | 20.7 | 12.8 | 2.03 | 0.68 | 0.48 | 2.07 | 7.25 | 0.80 | 0.07 | 0.08 | 187 | 33 | 94 | 30 | 107 | 71 | 100.0 |

trend can be interpreted in two ways: (1) by uplift and gradual erosion and recession of the source area, thereby reducing gradients and sediment supply and increasing the proportion of fine-grained material supplied to the depositional site, or (2) by increased rates of subsidence and vertical aggradation, which would tend to preserve more fines as the rate of channel reworking decreased. Unfortunately there is insufficient data from Hole 740A to assess the relative merits of these two mechanisms, although both may be related if fault controlled. Under these conditions the channels would tend to become more sinuous in character as the amount of silt and mud in the channel bed and bank increased (Schumm, 1960). The sediments were deposited by a network of shallow, low-sinuosity braided channels draining a vegetated alluvial plain (cf. Truswell, 1982) with sufficient topographic relief to trap fine-grained sediments and inhibit rapid channel shifting. Comparison of the channel deposits to the models of Miall (1977) and Rust (1978) suggests that the channels drained the intermediate parts of a braided river system, the proximal reaches of which probably existed toward the east and southeast, in the direction of the basement source area. Coarser grained braided river deposits may be present in this direction, with alluvial fans flanking the fault-bounded source area. Palynological studies by Truswell (1982) of seafloor samples dredged from off the East Antarctic coast suggest that well-vegetated alluvial plains were extensively developed over parts of East Antarctica prior to continental breakup. However, the only record of these sequences found to date is the locally preserved onshore Permian Amery Group and the Prydz Bay red beds. Similar sequences are predicted to occur farther south along the East Antarctic continental margin (Truswell, 1982).

Because of the relative stability of the channels, pedogenic processes were initiated on the vegetated flood plain. Most paleosols show up as mottled zones in the succession and are attributed to alternate wetting and drying of the soil by fluctuations in the level of the water table. Although the climate was warm, it was probably too wet for extensive calcrete formation and the development of mature soil profiles. Petrographic studies indicate that the sediments may have been derived from the upper Proterozoic and Archaean gneisses of the Prydz Bay coast, to the east and southeast of Hole 740A, which, like the sediments, have anomalously high concentrations of Cr and Ni. No other gneisses in this vicinity show the same geochemical signature. Additional evidence in support of this interpretation is provided by the seismic data, which show that the preglacial sediments at Prydz Bay form part of a much thicker sequence that progrades seaward (Stagg, 1985; Cooper and Larsen, 1989). Carbonate is present in the source rocks, but only in minor amounts (Ravich and Federov, 1982), and there is a decrease in the amount of CaO with decreasing age, which reflects a change in the relative abundance of plagioclase and potassium feldspar (Sheraton et al., 1984). In view of this, the paucity of carbonate in the sediments might also reflect a source area control on calcium availability to the depositional system as well as a climatic one. Tectonic activity and uplift of the source area probably occurred along the seaward extension of the eastern faulted margin of the Lambert Graben, which according to the seismic data (Stagg, 1985) passes to the southeast of Hole 740A. If this interpretation is correct, then the upper Proterozoic and Archaean gneisses of the Prydz Bay coast must extend seaward, at least as far as the eastern faulted margin of the Lambert Graben

(cf. Stagg, 1985, fig. 12). According to the available seismic data the boundary fault on the eastern side of the graben is a normal fault.

Palynological analysis of seven samples from this site has failed to resolve the age of the sediments (Truswell, this volume). Thus, their age is uncertain, although it has been suggested that they may be equivalent to the onshore Permian Amery Group or possibly younger (Stagg, 1985). The Amery Group attains a maximum thickness of about 270 m and consists of the Radok Conglomerate at the base, overlain by the Bainmedart Coal Measures and the Flagstone Bench Formation. The succession was deposited within a fluvial environment, but with the possibility of a glacial influence on sedimentation during deposition of the Radok Conglomerate (R. Tingey in Stagg, 1985). Recent work on the Amery Group has failed to substantiate Tingey's claim (B. McKelvey, pers. comm., 1989), and the Radok Conglomerate is considered to have been deposited by braided streams draining an alluvial fan system flanking the western faulted margin of the Lambert Graben. Sediment was derived from the nearby upper Proterozoic gneisses, granulites, and carbonate-rich metasediments to the west and southwest of the depositional site (cf. Mond, 1972). The Flagstone Bench Formation may be lithologically equivalent to the red beds that lie above the youngest Permian coals in Australia (Truswell, 1982). Furthermore, it is the only formation in the Amery Group to show any similarity to the Prydz Bay red beds. It consists of coarse-grained, cross-bedded, pebbly feldspathic sandstone and sandy siltstone arranged in vertically stacked fining-upward sequences. The coarser grained sandstones are light gray in color; the finer grained sandstones and siltstones are more reddish brown and variegated (Ravich et al., 1984). The major petrographic differences between the Amery Group sandstones and the Prydz Bay sandstones are that (1) they contain less biotite, (2) garnet is rare (generally only one grain per slide), and (3) carbonate (calcite and siderite) is abundant and may replace some of the feldspar, quartz, and clay matrix (Mond, 1972; B. McKelvey, pers. comm., 1989). These differences probably reflect source areas of different composition and have no bearing on the age relation between the two sequences. The Amery Group is generally considered to be late Permian in age (Mond, 1972; Kemp, 1973), although an early Permian age was assigned to the Radok Conglomerate by Ravich et al. (1977).

Seismic data indicate that the prebreakup sequence at Prydz Bay is 2–3 km thick and of early Permian to Early Cretaceous age (Stagg, 1985). Mond (1972) and Ravich and Federov (1982) correlated the upper Permian Amery Group with the Permo-Triassic Beacon Supergroup of the Transantarctic Mountains. Keating and Sakai (this volume) also suggested that the Prydz Bay red beds form part of the Permo-Triassic Beacon Supergroup on the basis of their similar lithologic relationships and magnetic characteristics. However, no primary component of Permian magnetization was isolated in their study, which revealed the presence of a thermomagnetically induced magnetic overprint attributed to Jurassic igneous intrusions. The possible presence of igneous intrusions in the Prydz Bay succession was first suggested by Stagg (1985). The preservation of Beacon Supergroup rocks within the Wilkes Basin on the East Antarctic coast south of Prydz Bay was postulated by Steed and Drewry (1982). However, palynological studies of dredged seafloor samples indicate that any Permian sediments that may exist in this part of East Antarctica have not been deeply buried or subjected to thermal metamorphism associated with igneous intrusions (Truswell, 1982; cf. Keating and Sakai, this volume).

ACKNOWLEDGMENTS

My thanks to the Ocean Drilling Program for the invitation to participate in Leg 119 and to the U.K. Natural Environmen-

tal Research Council for financial support. The diagrams were drafted by Christine Jeans, and the final version of the manuscript word-processed by Elizabeth Walton, Pat Bell, and Yvonne Hall, to whom I am most grateful.

REFERENCES

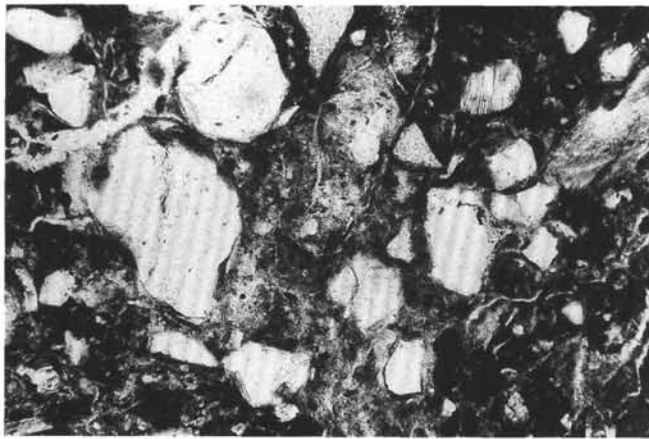
- Allen, J.R.L., 1974. Sedimentology of the Old Red Sandstone (Siluro-Devonian) in the Cleve Hills area, Shropshire, England. *Sediment. Geol.*, 12:73–167.
- , 1983. *Sedimentary Structures: Their Character and Physical Basis*: Amsterdam (Elsevier).
- Barron, J., Larsen, B., et al., 1989. *Proc. ODP, Init. Repts.*, 119: College Station, TX (Ocean Drilling Program).
- Brown, T. M., and Krause, M. J., 1981. Lower Eocene alluvial palaeosols (Willwood Formation) and their significance for palaeoecology, palaeoclimatology and basin analysis. *Palaeogeogr. Palaeoclimatol. Palaeoecol.*, 34:1–30.
- Collinson, J. D., and Thompson, D. B., 1982. *Sedimentary Structures*: London (Allen and Unwin).
- Cooper, A. K., and Larsen, B., 1989. Stratigraphy of Prydz Bay, Antarctica: preliminary results of ODP Leg 119 drilling. *Abst. Annu. AAPG Meeting*, San Antonio. (Abstract)
- de Raaf, J.F.M., Boersma, J. R., and Van Gelder, A., 1977. Wave generated structures and sequences from a shallow marine succession, lower Carboniferous, County Cork, Ireland. *Sedimentology*, 24: 451–483.
- Elliott, T., 1974. Abandonment facies of high constructive lobate deltas, with an example from the Yoredale Series. *Proc. Geol. Assoc.*, 85:359–365.
- Folk, R. L., 1968. *Petrology of Sedimentary Rocks*: Austin (Hemphill).
- Jopling, A. V., 1965. Laboratory study of sorting processes related to flow separation. *J. Geophys. Res.*, 69:3403–3118.
- Kemp, E. M., 1973. Permian flora from the Beaver Lake area, Prince Charles Mountains, Antarctica. I. Palynological examination of samples. *Bull. Bur. Miner. Resour. Geol. Geophys. Aust.*, 126:7–12.
- Leeder, M. R., 1975. Pedogenic carbonates and flood sediment accretion rates: a quantitative model for alluvial arid-zone lithofacies. *Geol. Mag.*, 112:257–270.
- Miall, A. D., 1977. A review of the braided-river depositional environment. *Earth Sci. Rev.*, 13:1–62.
- , 1985. Architectural-element analysis: a new method of facies analysis applied to fluvial deposits. *Earth Sci. Rev.*, 22:261–308.
- Mond, A., 1972. Permian sediments of the Beaver Lake area, Prince Charles Mountains. In Adie, R. J. (Ed.), *Antarctic Geology and Geophysics*: Oslo (Universitetsforlaget), 585–589.
- Pettijohn, F. P., Potter, P. E., and Siever, R., 1987. *Sand and Sandstones* (2d ed.): New York (Springer-Verlag).
- Ravich, M. G., and Federov, L. V., 1982. Geological structure of Mac-Robertson Land and Princess Elizabeth Land, East Antarctica. In Craddock, C. (Ed.) *Antarctic Geoscience*: Madison, WI (Univ. of Wisconsin Press), 499–504.
- Ravich, M. G., Gor, Y. G., Dibner, A. F., and Lobanova, O. V., 1977. Stratigrafia verknepaleozoiskikh ugleosnykh otlozhenii Vostochnoi Antarkidy (raion ozera River). [The stratigraphy of upper Paleozoic coal measures (Beaver Lake area, East Antarctica).] *Antarktika Doklady Kommissii*, 16:62–75.
- Ravich, M. G., Solov'ev, D. S., and Federov, L. V., 1984. *Geological Structure of Mac. Robertson Land (East Antarctica)*: New Delhi (Amerind Publ.), 56–69. [Translated from Russian and published for the Division of Polar Programs, National Science Foundation, Washington, DC]
- Reeves, C. C., Jr., 1970. Origin, classification, and geological history of caliche on the southern high plains, Texas and eastern New Mexico. *J. Geol.*, 79:352–362.
- Rust, B. R., 1978. Depositional models for braided alluvium. In Miall, A. D. (Ed.), *Fluvial Sedimentology*. Can. Assoc. Petrol. Geol. Mem., 5:605–626.
- Schumm, S. A., 1960. The effect of sediment type on the shape and stratification of some modern fluvial deposits. *Am. J. Sci.*, 258:177–184.
- Sheraton, J. W., Black, L. P., and McCulloch, M. T., 1984. Regional geochemical and isotopic characteristics of high-grade metamorphics of the Prydz Bay area: the extent of Proterozoic reworking of Ar-

- chaean continental crust in East Antarctica. *Precambrian Res.*, 26: 169-198.
- Stagg, H.M.J., 1985. The structure and origin of Prydz Bay and MacRobertson Shelf, East Antarctica. *Tectonophysics*, 114:315-340.
- Steed, R.H.N., and Drewry, D. J., 1982. Radio echo-sounding investigations of Wilkes Land, Antarctica. In Craddock, C. (Ed.), *Antarctic Geoscience*: Madison, WI (Univ. of Wisconsin Press), 969-975.
- Truswell, E. M., 1982. Palynology of seafloor samples collected by the 1911-14 Australian antarctic expedition: implications for the geology of coastal East Antarctica. *J. Geol. Soc. Aust.*, 29:343-356.
- Tunbridge, I. P., 1984. Facies model for a sandy ephemeral stream and clay playa complex: the middle Devonian Trentishoe Formation of North Devon, U.K. *Sedimentology*, 31:697-716.
- Turner, B. R., 1978. Sedimentary patterns of uranium mineralization in the Beaufort Group of the southern Karoo (Gondwana) Basin, South Africa. In Miall, A. D. (Ed.), *Fluvial Sedimentology*. Can. Assoc. Petrol. Geol. Mem., 5:831-848.
- Turner, P., 1980. *Continental Red Beds*: Amsterdam (Elsevier).

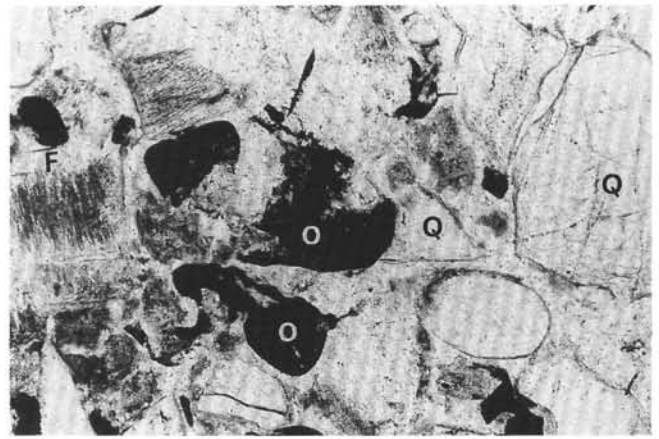
Date of initial receipt: 18 December 1989

Date of acceptance: 5 July 1990

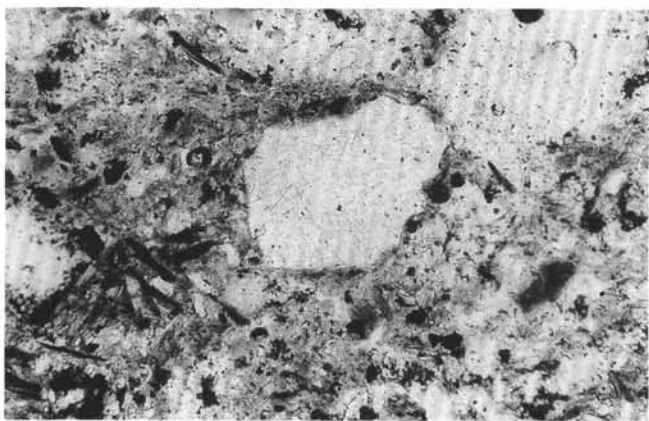
Ms 119B-133



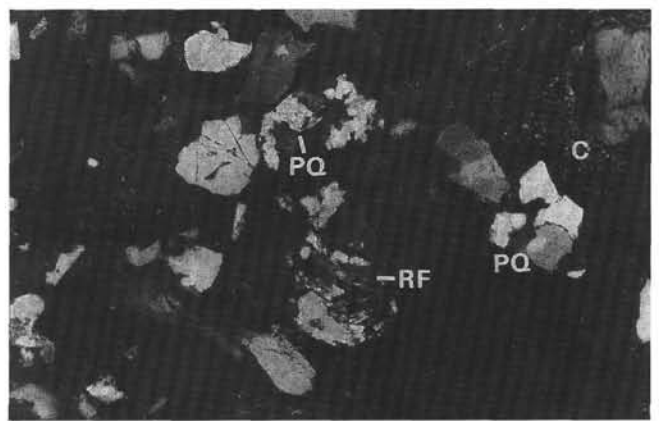
1 500μm



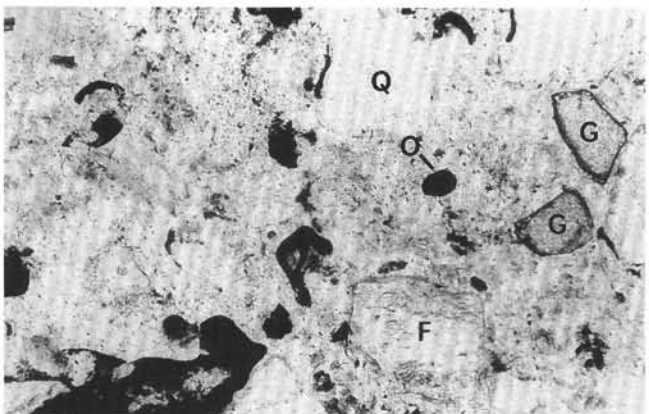
2 250μm



3 250μm



4 1mm



5 250μm



6 500μm

Plate 1. Thin-section photomicrographs of arkosic wackes from Hole 740A. 1. Poorly sorted, immature, coarse arkosic wacke comprising rounded to angular quartz grains and fresh to slightly altered feldspar set within a chlorite-rich clay matrix. Sample 119-740A-8R-5, 15-17 cm. Crossed nicols. 2. Well-rounded, recycled quartz grain associated with angular quartz grains (Q), orthoclase feldspar (F), and black opaque minerals (O). The large quartz grain at bottom right contains abundant needlelike inclusions of ?sillimanite. Sample 119-740A-17R-1, 100-103 cm. Plane polarized light. 3. Sillimanite needles in a quartz grain showing corroded margins. The clay matrix is rich in fine shreds of chlorite. Sample 119-740A-23R-1, 102-106 cm. Plane polarized light. 4. Quartz-micaceous-chlorite rock fragment (RF), polycrystalline quartz grains (PQ), and claystone clast (C). Sample 119-740A-17R-1, 100-103 cm. Crossed nicols. 5. Angular garnet grains (G), feldspar (F), quartz (Q), and opaque minerals (O). Sample 119-740A-17R-1, 100-103 cm. Plane polarized light. 6. Heavy mineral-rich laminae containing garnet and opaque ilmenite and titanomagnetite. Sample 119-740A-14R-1, 99-102 cm. Plane polarized light.